Letter

Excitatory-inhibitory branching process: A parsimonious view of cortical asynchronous states, excitability, and criticality

Roberto Corral López,[1] Víctor Buendía,[2,3] and Miguel A. Muñoz[1]

[1]*Departamento de Electromagnetismo y Física de la Materia and Instituto Carlos I de Física Teórica y Computacional, Universidad de Granada, E-18071 Granada, Spain*

[2]*Department of Computer Science, University of Tübingen, 72076 Tübingen, Germany,*

[3]*Max Planck Institute for Biological Cybernetics, 72076 Tübingen, Germany*

(Received 30 March 2022; revised 6 July 2022; accepted 13 October 2022; published 14 November 2022)

The branching process is the minimal model for propagation dynamics, avalanches, and criticality, broadly used in neuroscience. A simple extension of it, adding inhibitory nodes, induces a much-richer phenomenology, including an intermediate phase, between quiescence and saturation, that exhibits the key features of "asynchronous states" in cortical networks. Remarkably, in the inhibition-dominated case, it exhibits an extremely rich phase diagram that captures a wealth of nontrivial features of spontaneous brain activity, such as collective excitability, hysteresis, tilted avalanche shapes, and partial synchronization, allowing us to rationalize striking empirical findings within a common and parsimonious framework.

DOI: 10.1103/PhysRevResearch.4.L042027

The idea that information-processing systems, both biological and artificial, can extract important functional advantages from operating near the edge of a phase transition was already suggested by Turing in 1950, inspiring since then theory and experiment [1,2]. Beggs and Plenz, pioneering the experimental search for signatures of criticality in neural systems, found scale-free outbursts of neuronal activity occurring in between consecutive periods of quiescence, i.e., *neuronal avalanches* [3], as consistently reported across brain regions, species, and observational scales [3–9]. These avalanches have sizes and durations distributed as power laws with exponents consistent with those of a critical branching process (BP) [10,11] and often exhibit a parabolic shape on average (another trademark of critical BPs) [12–15]. In spite of some methodological caveats [16–18], experimental discrepancies [19], and the existence of alternative interpretations [20–23], the empirical observation of scale-free neuronal avalanches triggered renewed interest in the idea of criticality in brain networks [24–27] and its potential relevance for computation and information processing [28–31] (see also [1,2,32–34]). Nevertheless, the stylized picture of neuronal activity as a BP seems exceedingly naive, as it overlooks the fact that about 20% of the neurons in the cortex are inhibitory ones [35] and that these play a crucial role in shaping cortical activity [36–38]. Actually, the "standard model" of spontaneous brain activity is that of a "*balanced state*" in which excitatory and inhibitory inputs to any given neuron nearly cancel each other on average, giving rise to a fluctuation-dominated "*asynchronous state*" [39–42]. This is characterized by rather irregular (Poisson-like) single-neuron activations, delayed correlations between excitation and inhibition, and small averaged pairwise correlations, etc. [36,43–45]. These properties, important for efficient encoding of information [36–38,43], are markedly different from those of usual critical states but are also crucial for information processing, suggesting that critical and asynchronous states could act complementarily to tackle diverse functional tasks (e.g., requiring either strong correlation for collective response or decorrelation to limit redundancy). Hence describing these alternative states under a common overarching framework is a timely and challenging goal [45–51].

Here, we analyze what happens in archetypical models of activity propagation—such as the BP or, more specifically, its continuous-time counterpart: the contact process [10,11]—if, as sketched in Fig. 1, inhibitory units are considered in addition to the usual excitatory ones. Do additional phases beside the standard "quiescent" and "active" ones emerge [52–54]? What are their key features and phase transitions? In what follows we answer these questions, elucidating an extremely rich phenomenology that reproduces the key features of "asynchronous states," but also collective excitability, bistability, nonparabolic avalanches, quasioscillations, criticality, etc., allowing us to rationalize a wealth of striking empirical observations in a parsimonious way.

The excitation-inhibition contact process (EI-CP) is a generalization of the ordinary contact process (CP) [10,11,52–54], operating on top of an arbitrary directed network in which active excitatory neurons attempt to propagate activity to their neighbors, while inhibitory ones hinder such a propagation [35]. We consider diverse types of network architectures, such as fully connected graphs, sparse random networks, and two-dimensional (2D) lattices [see Fig. 1(c)].

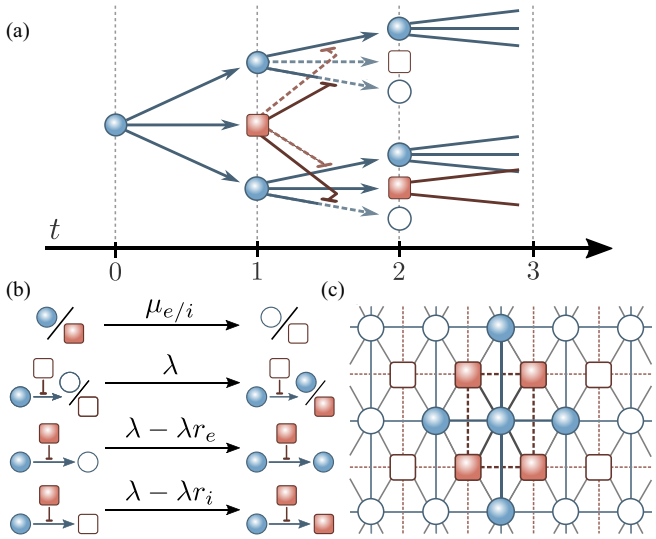

FIG. 1. (a) Sketch of an excitatory-inhibitory branching process on a tree; active inhibitory units (red squares) reduce the probability of propagation from active excitatory units (blue circles). Empty symbols stand for inactive units and full/dashed lines for fulfilled/unfulfilled processes. (b) Transition rates for the "excitatory-inhibitory contact process" (EI-CP). (c) Illustration of a two-dimensional (2D) lattice with a central cluster of active nodes.

The networks consist of N nodes, of which a fraction α are excitatory (E) and the remaining $(1-\alpha)N$ are inhibitory (I), a proportion that is preserved for the inward connectivity of every single node. The state of each node j at time t is defined by a binary variable [$s_j(t) = 1$ for active nodes and $s_j(t) = 0$ for inactive or "silent" ones] and $\rho_e(t)$ [$\rho_i(t)$] is the fraction of active excitatory (inhibitory) nodes. The dynamics is akin to the ordinary CP: active nodes become silent at a fixed rate $\mu_e = \mu_i = 1$, but only active *excitatory* nodes can propagate activity to each of their silent nearest neighbors at a rate λ/K. On the other hand, each active inhibitory node reduces the rate at which each neighbor is activated by $r_{e/i}\lambda/K$ (for E/I units, respectively), with $0 \leqslant r_{e/i} \leqslant 1$ [Fig. 1(a)]. Thus the activation rate of a silent node j is $f(\frac{\lambda}{K}\sum_{k\in\Omega_j^e} s_k - \frac{\lambda r_{(e/i)}}{K}\sum_{k\in\Omega_j^i} s_k)$, where $\Omega_j^{e/i}$ is the set of E/I neighbors of node j in the considered network, and the gain function, $f(\Lambda) = \max(0, \Lambda)$, enforces the non-negativity of the transition rates. We focus on the *asymmetric* variant of the model, in which inhibition acts more strongly on excitatory than on inhibitory nodes, i.e., $r \equiv r_e > r_i$, leading to *inhibition-dominated* networks. For simplicity, here we fix $r_i = 0$—i.e., no inhibition to inhibitory nodes—and $\alpha = 1/2$ [see Supplemental Material (SM) [55] for generalizations]. The master equation defined by the above rates can be integrated in an exact way with Gillespie's algorithm [56] and also studied analytically (see SM [55]).

Let us first discuss the case of fully connected networks, for which mean-field equations (exact in the infinite-N limit) can be derived from a standard size expansion [52,53,57],

$$\begin{aligned}\dot{\rho}_e(t) &= -\rho_e + (\alpha - \rho_e) f(\lambda(\rho_e - r\rho_i)),\\ \dot{\rho}_i(t) &= -\rho_i + (1 - \alpha - \rho_i) f(\lambda\rho_e),\end{aligned} \tag{1}$$

while for finite N, additional (demographic) noise terms need to be added to Eqs. (1) (see SM [55]). Notice that Eq. (1) is a version of the celebrated Wilson-Cowan model for neural dynamics [58,59] and that, actually, our full model is also a variant of the "stochastic Wilson-Cowan model," for which many illuminating results have been obtained in the *symmetric case* [46,60–62]. However, here we focus on the inhibition-dominated *asymmetric case*, which exhibits a much richer phenomenology (see below).

Observe that, owing to the piecewise definition of f, Eq. (1) is a nonsmooth dynamical system [63] and the space of states (ρ_e, ρ_i) is divided into (i) a *zone 1*, with $\rho_e - r\rho_i < 0$, for which the gain function in the equation for $\dot{\rho}_e(t)$ vanishes so that the quiescent state $\rho_e = \rho_i = 0$ is always reached, and (ii) a *zone 2*, for $\rho_e - r\rho_i > 0$ which—as shown in Fig. 2—entails a rich phase diagram including a quiescent phase, an active one, and a regime of bistability [the corresponding nullclines, fixed points, and characteristic trajectories are shown in Figs. 2(e)–2(h); see also [58,59,64]]. Observe that the transition from active to quiescent can be either (i) continuous, as in the standard CP [line of transcritical bifurcations at $\lambda_1(r) = \frac{4}{1+\sqrt{1-4r}}$ for $r \leqslant 1/4$; red line in Fig. 2(a)], (ii) discontinuous with bistability [saddle-node bifurcations at $\lambda_3(r) = \frac{8r}{(r-1)^2}$; blue line in Fig. 2(a), or (iii) *tricritical* at their merging point ($r_t = \sqrt{5} - 2$; yellow star). Note also the presence of a line of Hopf bifurcations [$\lambda_2(r) \equiv 4$ for $r \geqslant 1/4$; red horizontal dashed line], where the quiescent state loses its local stability, suggesting the emergence of oscillations above it. However, the nonsmoothness of the dynamical system leads to *frustrated oscillations*, i.e., excitatory perturbations (in zone 2) give rise to curved trajectories that cross to states in zone 1 and then decay back to quiescence [see Fig. 2(g)]. This generates an "*excitable phase*" above the Hopf line where the quiescent state is *locally unstable* to excitatory perturbations, so that these can be hugely amplified before relaxing back to quiescence, making it *globally stable*. This creates a mechanism for bursting/avalanching behavior, related to but different from the one studied in [46,60]. This type of transient-amplification effect is well known to stem from the non-normal (non-Hermitian) form of the Jacobian matrix and its implications have long been studied in neuroscience [46,58,65,66]. A particularly interesting case of non-normality occurs where the transcritical and Hopf lines meet, i.e., at the codimension-2 Bogdanov-Takens (BT) bifurcation [64], characteristic of, so-called, *nonreciprocal phase transitions*, a currently hot research topic [67]. The non-normal nature of the dynamics entails a number of nontrivial features such as tilted avalanches—characterized by a highly nonparabolic averaged shape as shown in Fig. 3—which appear all across the excitable phase when excitatory inputs perturb the quiescent state. Note that they are not scale invariant, i.e., they have diverse, duration-dependent, shapes (see also [61]). It is only at the line of continuous transitions that avalanches are both tilted and scale free, resembling the nonparabolic scale-free avalanches reported in, e.g., zebra-fish experiments [20]. Avalanches become parabolic only when inhibition is switched off ($r = 0$) and their scaling differs from the standard BP only at the exceptional BT point (its "exotic" critical features will be scrutinized elsewhere [68]). Thus, in summary, the asymmetric (inhibition-dominated) EI-

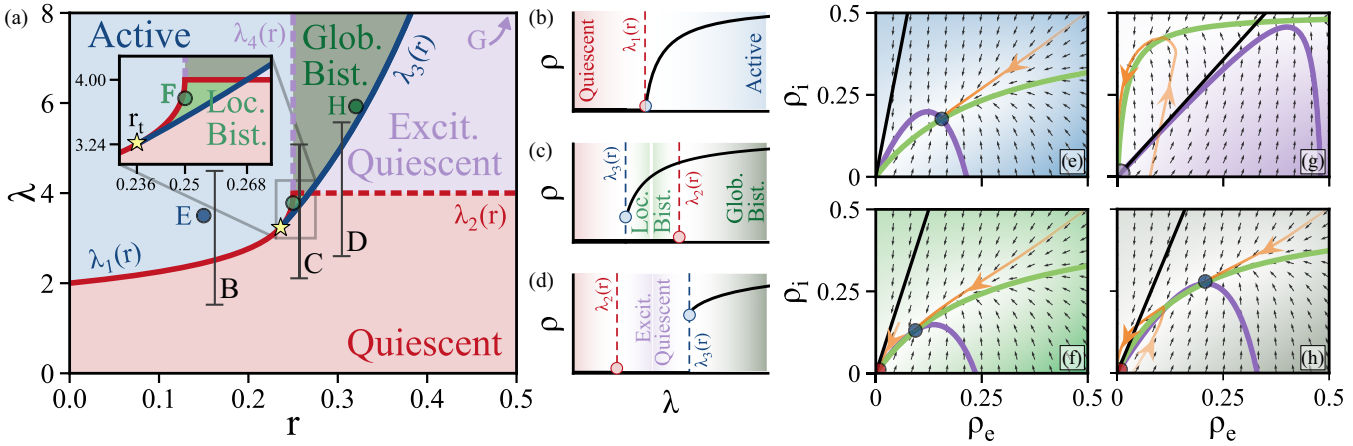

FIG. 2. Results for the excitatory-inhibitory contact process (EI-CP) on fully connected networks as analytically obtained from Eq. (1) for $\alpha = 1/2$, $r_i = 0$, and excitation-dominated initial conditions (note that inhibition-dominated conditions always lead to the quiescent state). (a) Phase portrait in the r-λ plane: Active phase (blue), quiescent phase (red), *excitable quiescent* phase (purple), and bistable regimes (green). The full red line $\lambda_1(r)$ [$\lambda_3(r)$ in blue] marks continuous (discontinuous) transitions between quiescent and active states. These two lines come together at a tricritical point (yellow star). The line $\lambda_2(r)$ marks a Hopf bifurcation, separating the standard quiescent phase from an excitable quiescent one, where the quiescent state is locally unstable, but globally stable. (b)–(d) Overall stationary activity $\rho = \rho_e + \rho_i$ as a function of λ for three different values of r as marked and color coded in (a): Continuous transition (b), discontinuous transition with a regime of bistability between an active state and a quiescent state (c), or between an active and an excitable quiescent state (d). (e)–(g) Flow diagrams in the ρ_e, ρ_i plane for the three points marked in panel (a); the background color stands for the phase and its color intensity is proportional to the vector-field module, the colored lines are the nullclines $\dot{\rho}_e = 0$ (green) and $\dot{\rho}_i = 0$ (purple), respectively, and the black line ($\rho_i = \rho_e/r$) separates zone 1 (inhibition dominated) from zone 2 (excitation dominated). Characteristic trajectories are depicted as arrowed orange lines, while colored points stand for stable steady states.

CP model exhibits a much-richer phenomenology than its standard CP counterpart (and that of the symmetric version of the model; see SM [55]) already at a mean-field level.

To go beyond mean field, we now study sparse networks ($K \ll N$) and scrutinize the effects of their inherent stochasticity. In particular, we start by considering analytically tractable *annealed random networks*—in which the αK excitatory and $(1-\alpha)K$ inhibitory neighbors of each single node are randomly selected at each time step. In this way, the input to each neuron is a random variable, whose probability distribution can be straightforwardly seen to be the product of two binomials (see SM [55]). From this probability distribution, one can then compute the mean activation rate for each node, $\langle f(\rho_e, \rho_i)\rangle_K$, which—as a consequence of Jensen's inequality [49]—turns out to be larger than its mean-field counterpart $f(\langle\rho_e\rangle_K, \langle\rho_i\rangle_K)$ in Eq. (1). The resulting exact equation can be solved using series expansions or numerically (see SM [55]). The most salient feature of its associated phase diagram [Fig. 4(a)] is the emergence of an intermediate phase between the standard quiescent and active phases. It is separated from the former by a line of continuous transitions [$\lambda_c(r) = 2$] and from the latter by either a sharp discontinuous transition with bistability for large values of r or by a smooth transition for small r's [Fig. 4(a)]. Observe that fluctuations, stemming from network sparsity, have blurred away the line of mean-field Hopf bifurcations as well as the BT point, so that the resulting intermediate phase is reminiscent of the mean-field excitable phase but, crucially, with a nonvanishing irregular activity (see below).

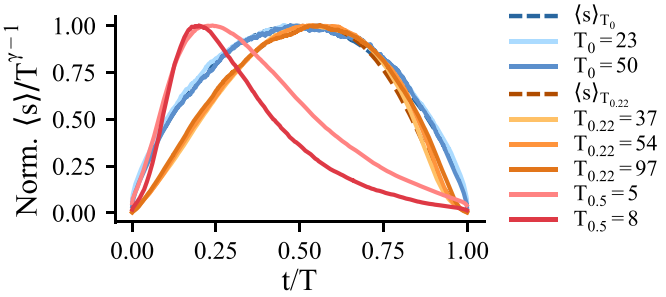

FIG. 3. Avalanche shapes rescaled with their duration T_r at different points of the mean-field phase diagram (characterized by r). Simulations are performed for the noisy version of Eq. (1) with small excitatory initial conditions (see SM-IV.B [55]). (i) At the inhibition-free critical point (blue curves; $r = 0$ and $\lambda_c = 2$) avalanches for different durations, $T_{r=0}$, are scale free as their rescaled curves collapse onto a universal inverted-parabola shape using the BP exponent $\gamma = 2$ [13,15]. (ii) In the presence of inhibition, the curves at the critical point (orange curves; $r = 0.22$ and $\lambda_c = 3$) are scale invariant with BP exponents and they collapse onto a slightly "tilted" nonparabolic curve (see also [61]). (iii) Within the excitable phase (red curves; $r = 0.5$ and $\lambda = 10$), i.e., away from bifurcations, one observes duration-dependent (non-scale-invariant) skewed nonparabolic shapes.

Importantly, even if the phase diagram in Fig. 4(a) has been derived for annealed networks, qualitatively identical ones—albeit with shifted phase boundaries—can be computationally obtained for sparse networks with a fixed (quenched) architecture (such as 2D lattices and random regular networks) with the same values of K and α. Hence the forthcoming results are, in general, valid for all these types of networks.

First of all, we notice that the intermediate phase in Fig. 4 exhibits all the key features of cortical asynchronous

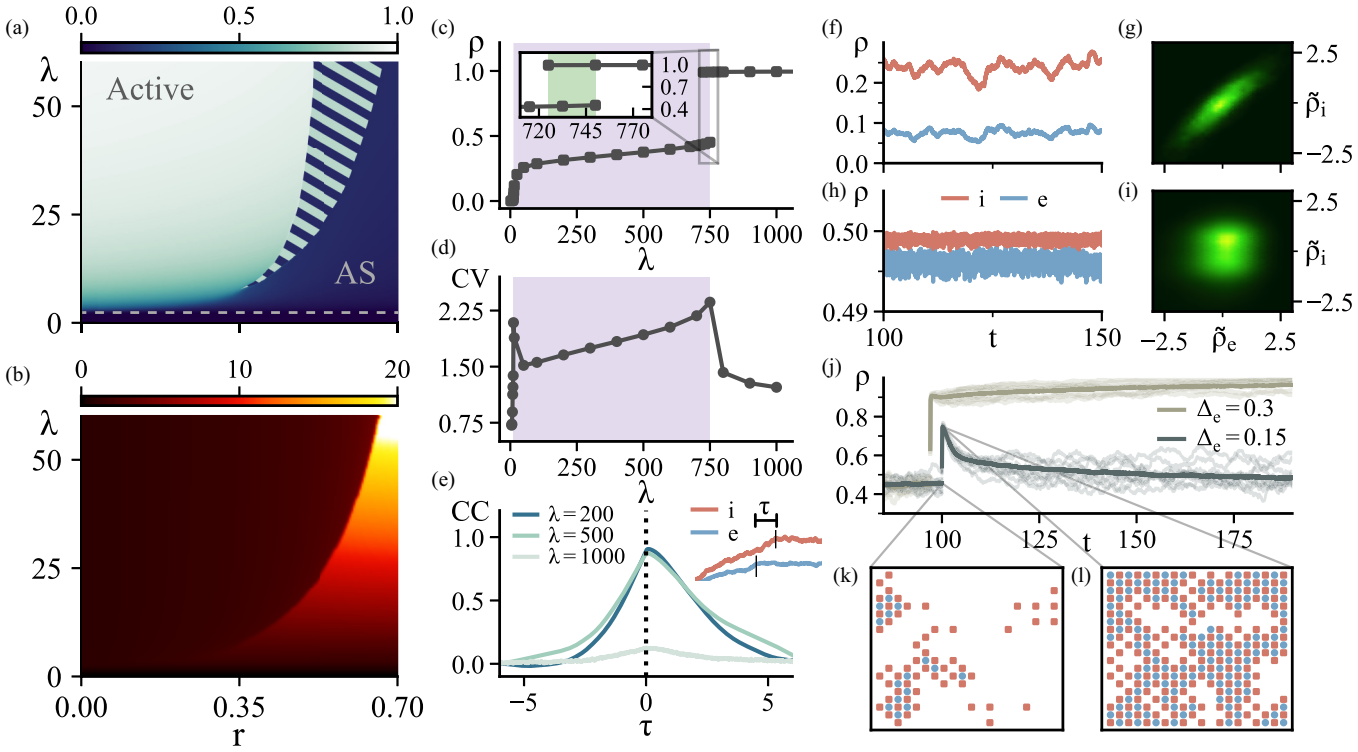

FIG. 4. Features of the asynchronous phase. (a),(b) Analytical results for sparse (annealed) random networks. (a) Stationary activity where the dashed line indicates the end of the quiescent phase and stripes signal the bistability region between the asynchronous and standard-active phase. (b) Henrici index gauging the level of non-normality in the r, λ diagram (see SM-IV.C [55]). (c)–(l) Results for a 2D lattice (which helps visualization) with $N = 10^4$. (c) Section of the phase diagram ($r = 0.7$), illustrating the discontinuous transition with bistability and (d) coefficient of variation (CV) for different values of λ. (e) Lagged cross correlations (CC) between excitatory and inhibitory time series; inhibition follows closely excitation with a delay τ. Total excitatory and inhibitory activity as a function of time for $r = 0.7$ is plotted in (f) for the AS phase ($\lambda = 200$) and in (h) for the standard active phase ($\lambda = 1000$); (g)–(i) same as in (f) and (h), respectively, plotted in the standardized $\tilde{\rho}_e$, $\tilde{\rho}_i$ plane (see SM-IV.C [55]), as an illustration of the diverse nature of cross correlations in both phases. (j) Stimulation experiment where a fraction Δ_e of excitatory nodes (on a 2D lattice) is transiently activated; in the bistability region ($r = 0.7$, $\lambda = 750$), this can potentially drive the system from the AS phase to the standard active phase, much as in experimental setups [72]. (k)/(l) Snapshots of the system before (k) and after (l) the perturbation ($N = 20^2$). See SM [55] for further details.

states [37,38,43,69,70], so we call it *asynchronous (AS) phase*. In particular, (i) the coefficient of variation (CV)—i.e., the ratio of the variance to the mean activity (see SM [55])—takes values $CV > 1$, as corresponds to highly irregular single-node activations [Fig. 4(d)], (ii) time series for inhibitory nodes tightly follow excitatory ones [Fig. 4(e)], leading to strong lagged cross correlations between excitation and inhibition [Figs. 4(f)/4(g)], a feature absent in the standard active phase [Figs. 4(h)/4(i)], and (iii) small averaged pairwise correlations are found (not shown). However, most remarkably, the elucidated AS phase—in the regime of large λ and r values—exhibits also important features characteristic of brain spontaneous activity that are typically not described by standard simple models of asynchronous states [43]. These include the following. *(A) Collective excitability.* As shown in Fig. 4(b), the AS phase is characterized by a large degree of non-normality—as quantified, e.g., by the Henrici index [71]—that grows with both λ and r. In this regime, the AS phase can be highly excitable as illustrated in Fig. 4(j), so those small perturbations can give rise to very large excursions far away from quiescence, generating large tilted avalanches. *(B) Bistability with hysteresis.* Given that the AS phase can coexist with the active one, it is feasible to shift the network dynamical regime from a low-activity (AS) to high-activity (standard active) one by perturbating the system above some threshold [see Fig. 4(j) and SM [55]]. This shift resembles the striking empirical observation that the collective state of the cortex can be shifted from a low-activity state to a stable active state with a relatively small perturbation [72]. Another consequence of bistability is the presence of hysteresis which is important for, e.g., working memory [73]. *(C) Partial synchronization.* As illustrated in the SM (Fig. S5) [55], there are quasioscillations, evinced as a peak in the Fourier transform of the activity time series [74,75], followed by a power-law decay revealing variable and transient levels of synchronization, as observed in the cortex [74]. Importantly, this phenomenology survives when inhibition to inhibitory neurons is switched on ($r_i \neq 0$), but tends to disappear as the symmetric limit ($r_i = r_e$) is approached (see SM [55]), providing a simple explanation of why "inhibition of inhibition" is often mild in brain networks, which are thus "inhibition dominated" [36] (cf. [76]).

Finally, we also confirmed computationally that the phase transition from the quiescent to the AS phase is described by the directed-percolation class (either in mean field or in 2D; see SM [55]). Violations of such uni-

versality occurring at special points will be described elsewhere [68].

In summary, the EI-CP—an extension of the archetypical contact process including additionally inhibitory nodes—exhibits an extremely rich phenomenology, especially in the inhibition-dominated case and on sparse networks. In particular, on these networks, one finds an AS phase that captures the basic features of asynchronous states in the brain, and also describes additional remarkable properties, such as collective excitability and partial synchronization, which are usually not explained by existing simple models of asynchronous states. In this way, the model allowed us to rationalize empirical observations, such as (i) scale-free tilted neuronal avalanches [20,77], (ii) regime shifts in the overall network state emerging after a limited perturbation [72], and (iii) quasioscillations [74], that are certainly well beyond the limit of validity of the standard BP picture, as well as simple models of asynchronous states [43]. Furthermore, this allows us to put under the same parsimonious setting critical states (including some exotic ones) and asynchronous states, paving the way towards a deeper understanding of the statistical mechanics of spontaneous brain activity. Extensions of our approach, including important features of actual neural networks, such as more heterogeneous network architectures, distributed synaptic weights, refractory periods, etc., will be explored elsewhere.

We acknowledge the Spanish Ministry and Agencia Estatal de investigación (AEI) through Project of I + D+i Ref. PID2020-113681GB-I00, financed by MICIN/AEI/10.13039/501100011033 and FEDER "A way to make Europe," as well as the Consejería de Conocimiento, Investigación Universidad, Junta de Andalucía and European Regional Development Fund, Project references A-FQM-175-UGR18 and P20-00173, for financial support. R.C.L. acknowledges funding from the Spanish Ministry and AEI, Grant No. FPU19/03887. This work was partially supported by a Sofja Kovalevskaja Award from the Alexander von Humboldt Foundation, endowed by the German Federal Ministry of Education and Research (V.B.). We also thank H. C. Piuvezam, J. Pretel, G. B. Morales, P. Moretti, O. Vinogradov, and E. Giannakakis for valuable discussions.

[1] T. Mora and W. Bialek, Are biological systems poised at criticality?, J. Stat. Phys. **144**, 268 (2011).

[2] M. A. Muñoz, Colloquium: Criticality and dynamical scaling in living systems, Rev. Mod. Phys. **90**, 031001 (2018).

[3] J. M. Beggs and D. Plenz, Neuronal avalanches in neocortical circuits, J. Neurosci. **23**, 11167 (2003).

[4] T. Petermann, T. C. Thiagarajan, M. A. Lebedev, M. A. Nicolelis, D. R. Chialvo, and D. Plenz, Spontaneous cortical activity in awake monkeys composed of neuronal avalanches, Proc. Natl. Acad. Sci. USA **106**, 15921 (2009).

[5] A. Haimovici, E. Tagliazucchi, P. Balenzuela, and D. R. Chialvo, Brain Organization into Resting State Networks Emerges at Criticality on a Model of the Human Connectome, Phys. Rev. Lett. **110**, 178101 (2013).

[6] E. Tagliazucchi, P. Balenzuela, D. Fraiman, and D. R. Chialvo, Criticality in large-scale brain fmri dynamics unveiled by a novel point process analysis, Front. Physiol. **3**, 15 (2012).

[7] O. Shriki, J. Alstott, F. Carver, T. Holroyd, R. N. Henson, M. L. Smith, R. Coppola, E. Bullmore, and D. Plenz, Neuronal avalanches in the resting MEG of the human brain, J. Neurosci. **33**, 7079 (2013).

[8] T. Bellay, A. Klaus, S. Seshadri, and D. Plenz, Irregular spiking of pyramidal neurons organizes as scale-invariant neuronal avalanches in the awake state, Elife **4**, e07224 (2015).

[9] S. Yu, T. L. Ribeiro, C. Meisel, S. Chou, A. Mitz, R. Saunders, and D. Plenz, Maintained avalanche dynamics during task-induced changes of neuronal activity in nonhuman primates, Elife **6**, e27119 (2017).

[10] T. Liggett, *Interacting Particle Systems*, Classics in Mathematics (Springer, Berlin, 2004).

[11] T. E. Harris, *The Theory of Branching Processes*, Grundlehren der mathematischen Wissenschaften (Springer Berlin, Heidelberg, 1963).

[12] J. P. Sethna, K. A. Dahmen, and C. R. Myers, Crackling noise, Nature (London) **410**, 242 (2001).

[13] N. Friedman, S. Ito, B. A. W. Brinkman, M. Shimono, R. E. L. DeVille, K. A. Dahmen, J. M. Beggs, and T. C. Butler, Universal Critical Dynamics in High Resolution Neuronal Avalanche Data, Phys. Rev. Lett. **108**, 208102 (2012).

[14] S. R. Miller, S. Yu, S. Pajevic, and D. Plenz, Long-term stability of avalanche scaling and integrative network organization in prefrontal and premotor cortex, Network Neurosci. **5**, 505 (2021).

[15] S. di Santo, P. Villegas, R. Burioni, and M. A. Muñoz, Simple unified view of branching process statistics: Random walks in balanced logarithmic potentials, Phys. Rev. E **95**, 032115 (2017).

[16] V. Priesemann, M. H. Munk, and M. Wibral, Subsampling effects in neuronal avalanche distributions recorded in vivo, BMC Neurosci. **10**, 40 (2009).

[17] M. Martinello, J. Hidalgo, A. Maritan, S. di Santo, D. Plenz, and M. A. Muñoz, Neutral Theory and Scale-Free Neural Dynamics, Phys. Rev. X **7**, 041071 (2017).

[18] V. Priesemann, M. Valderrama, M. Wibral, and M. Le Van Quyen, Neuronal avalanches differ from wakefulness to deep sleep–evidence from intracranial depth recordings in humans, PLoS Comput. Biol. **9**, e1002985 (2013).

[19] A. J. Fontenele, N. A. P. de Vasconcelos, T. Feliciano, L. A. A. Aguiar, C. Soares-Cunha, B. Coimbra, L. Dalla Porta, S. Ribeiro, A. J. Rodrigues, N. Sousa, P. V. Carelli, and M. Copelli, Criticality between Cortical States, Phys. Rev. Lett. **122**, 208101 (2019).

[20] A. Ponce-Alvarez, A. Jouary, M. Privat, G. Deco, and G. Sumbre, Whole-brain neuronal activity displays crackling noise dynamics, Neuron **100**, 1446 (2018).

[21] S. di Santo, P. Villegas, R. Burioni, and M. A. Muñoz, Landau–ginzburg theory of cortex dynamics: Scale-free avalanches emerge at the edge of synchronization, Proc. Natl. Acad. Sci. USA **115**, E1356 (2018).

[22] V. Buendía, P. Villegas, R. Burioni, and M. A. Muñoz, Hybrid-type synchronization transitions: Where incipient oscillations,

scale-free avalanches, and bistability live together, Phys. Rev. Res. **3**, 023224 (2021).
[23] B. Mariani, G. Nicoletti, M. Bisio, M. Maschietto, S. Vassanelli, and S. Suweis, Disentangling the critical signatures of neural activity, Sci. Rep. **12**, 10770 (2022).
[24] D. Plenz and E. Niebur, *Criticality in Neural Systems* (John Wiley & Sons, New York, 2014).
[25] D. R. Chialvo, Emergent complex neural dynamics, Nat. Phys. **6**, 744 (2010).
[26] A. Levina, J. M. Herrmann, and T. Geisel, Dynamical synapses causing self-organized criticality in neural networks, Nat. Phys. **3**, 857 (2007).
[27] L. J. Fosque, R. V. Williams-García, J. M. Beggs, and G. Ortiz, Evidence for Quasicritical Brain Dynamics, Phys. Rev. Lett. **126**, 098101 (2021).
[28] O. Kinouchi and M. Copelli, Optimal dynamical range of excitable networks at criticality, Nat. Phys. **2**, 348 (2006).
[29] W. L. Shew, H. Yang, T. Petermann, R. Roy, and D. Plenz, Neuronal avalanches imply maximum dynamic range in cortical networks at criticality, J. Neurosci. **29**, 15595 (2009).
[30] W. L. Shew and D. Plenz, The functional benefits of criticality in the cortex, Neuroscientist **19**, 88 (2013).
[31] Z. Ma, G. G. Turrigiano, R. Wessel, and K. B. Hengen, Cortical circuit dynamics are homeostatically tuned to criticality in vivo, Neuron **104**, 655 (2019).
[32] D. Plenz, T. L. Ribeiro, S. R. Miller, P. A. Kells, A. Vakili, and E. L. Capek, Self-organized criticality in the brain, Front. Phys. **9**, 639389 (2021).
[33] L. Cocchi, L. L. Gollo, A. Zalesky, and M. Breakspear, Criticality in the brain: A synthesis of neurobiology, models and cognition, Prog. Neurobiol. **158**, 132 (2017).
[34] J. Wilting and V. Priesemann, 25 years of criticality in neuroscience–established results, open controversies, novel concepts, Curr. Opin. Neurobiol. **58**, 105 (2019).
[35] P. Dayan and L. F. Abbott, *Theoretical Neuroscience: Computational and Mathematical Modeling of Neural Systems* (MIT Press, Cambridge, MA, 2006).
[36] J. S. Isaacson and M. Scanziani, How inhibition shapes cortical activity, Neuron **72**, 231 (2011).
[37] B. Doiron, A. Litwin-Kumar, R. Rosenbaum, G. K. Ocker, and K. Josić, The mechanics of state-dependent neural correlations, Nat. Neurosci. **19**, 383 (2016).
[38] S. Denéve and C. K. Machens, Efficient codes and balanced networks, Nat. Neurosci. **19**, 375 (2016).
[39] C. van Vreeswijk and H. Sompolinsky, Chaos in neuronal networks with balanced excitatory and inhibitory activity, Science **274**, 1724 (1996).
[40] N. Brunel, Dynamics of sparsely connected networks of excitatory and inhibitory spiking neurons, J. Comput. Neurosci. **8**, 183 (2000).
[41] N. Brunel and X.-J. Wang, What determines the frequency of fast network oscillations with irregular neural discharges? I. Synaptic dynamics and excitation-inhibition balance, J. Neurophysiol. **90**, 415 (2003).
[42] I. Ginzburg and H. Sompolinsky, Theory of correlations in stochastic neural networks, Phys. Rev. E **50**, 3171 (1994).
[43] A. Renart, J. De La Rocha, P. Bartho, L. Hollender, N. Parga, A. Reyes, and K. D. Harris, The asynchronous state in cortical circuits, Science **327**, 587 (2010).
[44] T. Sippy and R. Yuste, Decorrelating action of inhibition in neocortical networks, J. Neurosci. **33**, 9813 (2013).
[45] D. Dahmen, S. Grün, M. Diesmann, and M. Helias, Second type of criticality in the brain uncovers rich multiple-neuron dynamics, Proc. Natl. Acad. Sci. USA **116**, 13051 (2019).
[46] M. Benayoun, J. D. Cowan, W. van Drongelen, and E. Wallace, Avalanches in a stochastic model of spiking neurons, PLoS Comput. Biol. **6**, e1000846 (2010).
[47] J. Wilting, J. Dehning, J. Pinheiro Neto, L. Rudelt, M. Wibral, J. Zierenberg, and V. Priesemann, Operating in a reverberating regime enables rapid tuning of network states to task requirements, Front. Syst. Neurosci. **12**, 55 (2018).
[48] J. Liang, T. Zhou, and C. Zhou, Hopf bifurcation in mean field explains critical avalanches in excitation-inhibition balanced neuronal networks: a mechanism for multiscale variability, Front. Syst. Neurosci. **14**, 580011 (2020).
[49] V. Buendía, P. Villegas, S. di Santo, A. Vezzani, R. Burioni, and M. A. Muñoz, Jensen's force and the statistical mechanics of cortical asynchronous states, Sci. Rep. **9**, 15183 (2019).
[50] M. Girardi-Schappo, E. F. Galera, T. T. Carvalho, L. Brochini, N. L. Kamiji, A. C. Roque, and O. Kinouchi, A unified theory of e/i synaptic balance, quasicritical neuronal avalanches and asynchronous irregular spiking, J. Phys. Complex. **2**, 045001 (2021).
[51] J. Li and W. L. Shew, Tuning network dynamics from criticality to an asynchronous state, PLoS Comput. Biol. **16**, e1008268 (2020).
[52] J. Marro and R. Dickman, *Nonequilibrium Phase Transition in Lattice Models* (Cambridge University Press, Cambridge, UK, 1999).
[53] M. Henkel, H. Hinrichsen, and S. Lübeck, *Non-equilibrium Phase Transitions: Absorbing Phase Transitions*, Theoretical and Mathematical Physics (Springer, Berlin, 2008).
[54] G. Ódor, *Universality in Nonequilibrium Lattice Systems: Theoretical Foundations* (World Scientific, Singapore, 2008).
[55] See Supplemental Material at http://link.aps.org/supplemental/10.1103/PhysRevResearch.4.L042027 for a detailed derivation of the model, mean-field results, sparse networks analysis, and methods.
[56] D. T. Gillespie, Stochastic simulation of chemical kinetics, Annu. Rev. Phys. Chem. **58**, 35 (2007).
[57] R. Pastor-Satorras, C. Castellano, P. Van Mieghem, and A. Vespignani, Epidemic processes in complex networks, Rev. Mod. Phys. **87**, 925 (2015).
[58] J. D. Cowan, J. Neuman, and W. van Drongelen, Wilson–cowan equations for neocortical dynamics, J. Math. Neurosci. **6**, 1 (2016).
[59] E. Negahbani, D. A. Steyn-Ross, M. L. Steyn-Ross, M. T. Wilson, and J. W. Sleigh, Noise-induced precursors of state transitions in the stochastic wilson–cowan model, J. Math. Neurosci. **5**, 9 (2015).
[60] S. di Santo, P. Villegas, R. Burioni, and M. A. Muñoz, Non-normality, reactivity, and intrinsic stochasticity in neural dynamics: A non-equilibrium potential approach, J. Stat. Mech.: Theory Exp. (2018) 073402.
[61] A. de Candia, A. Sarracino, I. Apicella, and L. de Arcangelis, Critical behaviour of the stochastic wilson-cowan model, PLoS Comput. Biol. **17**,e1008884 (2021).

[62] A. Sarracino, O. Arviv, O. Shriki, and L. de Arcangelis, Predicting brain evoked response to external stimuli from temporal correlations of spontaneous activity, Phys. Rev. Res. **2**, 033355 (2020).
[63] M. Kunze, *Non-smooth Dynamical Systems* (Springer Science & Business Media, New York, 2000), Vol. 1744.
[64] E. M. Izhikevich, *Dynamical Systems in Neuroscience* (MIT Press, Cambridge, MA, 2007).
[65] B. K. Murphy and K. D. Miller, Balanced amplification: A new mechanism of selective amplification of neural activity patterns, Neuron **61**, 635 (2009).
[66] G. Hennequin, T. P. Vogels, and W. Gerstner, Non-normal amplification in random balanced neuronal networks, Phys. Rev. E **86**, 011909 (2012).
[67] M. Fruchart, R. Hanai, P. B. Littlewood, and V. Vitelli, Non-reciprocal phase transitions, Nature (London) **592**, 363 (2021).
[68] H. Piuvezam *et al.* (unpublished).
[69] D. Hansel and G. Mato, Existence and Stability of Persistent States in Large Neuronal Networks, Phys. Rev. Lett. **86**, 4175 (2001).
[70] B. Kriener, H. Enger, T. Tetzlaff, H. E. Plesser, M.-O. Gewaltig, and G. T. Einevoll, Dynamics of self-sustained asynchronous-irregular activity in random networks of spiking neurons with strong synapses, Front. Comput. Neurosci. **8**, 136 (2014).
[71] M. Asllani, R. Lambiotte, and T. Carletti, Structure and dynamical behavior of non-normal networks, Sci. Adv. **4**, eaau9403 (2018).
[72] C.-y. T. Li, M.-m. Poo, and Y. Dan, Burst spiking of a single cortical neuron modifies global brain state, Science **324**, 643 (2009).
[73] D. Durstewitz, J. K. Seamans, and T. J. Sejnowski, Neurocomputational models of working memory, Nat. Neurosci. **3**, 1184 (2000).
[74] E. Wallace, M. Benayoun, W. van Drongelen, and J. Cowan, Emergent oscillations in networks of stochastic spiking neurons, PLoS One **6**, e14804 (2011).
[75] J. Hidalgo, L. Seoane, J. Cortés, and M. Muñoz, Stochastic amplification of fluctuations in cortical upstates, PLoS One **7**, e40710 (2012).
[76] R. Kim and T. J. Sejnowski, Strong inhibitory signaling underlies stable temporal dynamics and working memory in spiking neural networks, Nat. Neurosci. **24**, 129 (2021).
[77] J. P. Gleeson and R. Durrett, Temporal profiles of avalanches on networks, Nat. Commun. **8**, 1227 (2017).